Brain (1996), **119**, 775–787

Selective loss of myelin-associated glycoprotein from myelin correlates with anti-MAG antibody titre in demyelinating paraproteinaemic polyneuropathy

J.-M. Gabriel,[1] B. Erne,[1] G. C. Miescher,[1] S. L. Miller,[3] A. Vital,[4] C. Vital[4] and A. J. Steck[2]

Departments of [1]Research and [2]Clinical Neurology, University Hospital Basel, Switzerland, the [3]Division of Neurology Research, Children's Hospital Philadelphia, USA and the [4]Service d'Anatomie Pathologique, Hôpital Pellegrin, Bordeaux, France

Correspondence to: A. J. Steck, Neurology Clinic, University Hospital Basel, Petersgraben 4, CH-4031 Basel, Switzerland

Summary

The IgM monoclonal autoantibodies of patients with demyelinating paraproteinaemic polyneuropathy recognize a carbohydrate structure present on both myelin-associated glycoprotein (MAG) and protein zero (P_0). These autoantibodies are sufficient to cause the disease but the mechanism of demyelination remains unclear. We have analysed nerve biopsies from eight patients with polyneuropathy and anti-MAG antibodies by quantitative immunohistochemistry and find a concordant pattern of reduced expression of myelin markers with the loss of myelinated fibres. We report here novel features of this disease, in particular a selective lack of detectable MAG in a large proportion of myelinated fibres containing P_0, myelin basic protein (MBP) and periaxin. There is also an inverse correlation of the distribution of MAG in peripheral nerve myelin with the serum anti-MAG antibody titres but no correlation of these titres with the loss of myelinated fibres. Double immunofluorescence staining of paraproteinaemic polyneuropathy (PPN) nerves shows anti-MAG IgM deposited on the periphery of myelinated fibres associated with or lacking MAG staining. These data suggest that the binding of anti-MAG antibodies to MAG and/or other myelin component(s) results in MAG downregulation and may have an essential role in the molecular mechanisms leading to demyelination and partial regeneration in this disease.

Keywords: myelin-associated glycoprotein; anti-MAG autoantibodies; paraproteinaemic polyneuropathy; enzyme immunohistochemistry; quantitative image analysis

Abbreviations: anti-MAG PPN = PPN cases with anti-MAG autoantibody activity; GalC = galactocerebroside; GFAP = glial fibrillary acidic protein; HNK-1, human natural killer cells-1 mAb; mAb = monoclonal antibody; MAG = myelin-associated glycoprotein; MBP = myelin basic protein; M-IgM = monoclonal immunoglobulin IgM; P_0 = myelin protein zero; PPN = paraproteinaemic polyneuropathy

Introduction

In a large proportion of patients with demyelinating peripheral PPN, monoclonal IgM antibodies (M-IgM) react primarily with the human natural killer cells-1 (HNK-1) carbohydrate determinant of MAG (Braun *et al.*, 1982; McGarry *et al.*, 1983; Schuller-Petrovic *et al.*, 1983; Steck *et al.*, 1983; Frail *et al.*, 1984), in addition to myelin glycolipids (Ilyas *et al.*, 1984) and P_0 (Bollensen *et al.*, 1988). Here we consider exclusively these cases associated with anti-MAG autoantibodies (anti-MAG PPN). The anti-MAG PPN is a slowly progressive disease with distally pronounced loss of sensory and motor functions (Kaku *et al.*, 1994). The main pathological features are demyelinating lesions and deposits of autoantibodies associated with a 23 nm spacing between the separated leaflets of the intermediate line that results in

a widening of the outer myelin lamellae (King and Thomas, 1984). These lesions are not associated with inflammatory cellular infiltrates or any signs of acute cytotoxicity. The mechanism of presumable alteration of the blood–nerve barrier is not known. There are compelling arguments for a causative role of the patient's anti-MAG M-IgM: (i) the injection of patient's anti-MAG M-IgM in chicks results in demyelination with characteristic widening of the myelin lamellae (Tatum, 1993); (ii) this ultrastructural alteration is the site where anti-MAG M-IgM deposits of the corresponding class of light chain have been localized (Mendell *et al.*, 1985; Monaco *et al.*, 1990; Lach *et al.*, 1993); (iii) intraneural injection of anti-MAG M-IgM in species expressing HNK-1-type carbohydrates causes focal demyelination (Trojaborg *et al.*, 1989). Nerve biopsies usually contain demyelinating lesions with active zones of remyelination, and sometimes axonal damage of variable severity (Vital *et al.*, 1989).

In order to get further insights into the pathogenesis of the anti-MAG M-IgM neuropathy we have looked for coordinate changes of various myelin components by quantitative immunohistochemistry and have analysed the expression and distribution of several myelin and non-myelin markers in biopsies of patients with anti-MAG M-IgM neuropathy. While we found a concordant pattern of reduced expression of myelin markers with the loss of myelinated fibres, the observation of a disproportional reduction of fibres with detectable MAG levels together with the finding of highly significant inverse correlation with the serum anti-MAG titres suggests that MAG is the major target of the M-IgM autoantibodies.

Material and methods

Tissue specimens

Peroneal nerve biopsies from eight patients with paraproteinaemic polyneuropathy and monoclonal anti-MAG IgM antibodies (Bo 1, –4, –6, –7, –9, –10, –11, –12) and three autopsy controls (two sural nerves and one peroneal nerve) without neurological disease were embedded in O.C.T. compound (Miles, Elkhart, Ind., USA) and snap frozen. The inclusion criteria for this study were anti-MAG antibody titres greater than 100 by Western blot analysis of CNS myelin and the absence of structural artifacts or high background staining in the nerve biopsies. All these patients were evaluated at the Department of Neurology, University Hospital of Bordeaux. They underwent routine EMG and nerve conduction studies. The peroneal nerve biopsies were studied by light and electron microscopy, while IgM deposits were demonstrated by direct immunofluorescence microscopy (Vital *et al.*, 1989).

Anti-MAG M-IgM titres

Myelin was isolated from human brain and human peripheral nerve (cauda equina) by sucrose gradient centrifugation, resolved by sodium dodecylsulphate–polyacrylamide gel electrophoresis and blotted to nitrocellulose membranes as described by Burger *et al.* (1990). Serial dilutions of patient's antibodies binding to MAG were assayed by Western blot analysis using 1:1000 anti-human IgM (Fc)-peroxidase (Nordic, Tilburg, Netherland) in blocking buffer (1.5 mg ml^{-1} casein, 0.2% Tween 20 in phosphate buffered saline) and Fast-DAB as substrate (Sigma). The antibody titre is given as the reciprocal of the highest serum dilution at which antibody binding to the 100 kDa protein band is detected.

Polyclonal and monoclonal antibodies

Myelin-associated glycoprotein and periaxin were selected as markers of early myelination, while P_0, MBP and galactocerebroside (GalC) antigens are myelin-specific markers appearing at later stages of myelination. The following antibodies to myelin specific proteins were used: D3A2G5 (Burger *et al.*, 1990) or 513 (Boehringer; Poltorak *et al.*, 1987) anti-MAG monoclonal antibodies (mAbs), P07 (Archelos *et al.*, 1993) or D4IE4 (Miller *et al.*, 1984) anti-P_0 mAbs, HNK-1 mAb (ATCC TIB 200; Abo and Balch, 1981), 130–137 anti-MBP mAb (Boehringer), anti-periaxin polyclonal (Gillespie *et al.*, 1994), and mGalC/D12 anti-GalC mAb (Boehringer). The antibodies against non-myelin proteins were: G-A-5 mAb (Boehringer; Debus *et al.*, 1983) or Z-334 (Dako) polyclonal anti-glial fibrillary acidic protein (GFAP), 15E2E2 mAb (Boehringer) or Z-311 (Dako) polyclonal anti-protein S-100, and NN18 anti-neurofilament 160 kDa mAb (Boehringer; Weber *et al.*, 1983).

Immunohistochemistry

Cryostat sections (7 μm thick) were mounted on gelatin–chromalum-coated slides and fixed with 10% v/v buffered formalin for 20 min. It was necessary to extend the fixation to 5 h and to add a mild lipid extraction step with 15% ethanol for 40 h to reliably detect molecules which are associated with the myelin membrane (MAG, P_0, MBP, HNK-1 and GalC). Cytoplasmic or non-myelinating Schwann cell markers did not require this step. Blocking of endogenous peroxidase activity was achieved in 80% methanol:19.4% water:0.6% H_2O_2 for 20 min at room temperature. Saturation of nonspecific binding sites was performed with a blocking buffer (1% v/v normal goat serum, 2% w/v fish skin gelatin, 0.25% v/v Triton X-100 in phosphate buffered saline) for 15 min at room temperature (Bergoffen *et al.*, 1993). The blocking and incubation procedures for MBP detection were performed without Triton X-100 to avoid detergent extraction of MBP. Prior to incubation, all antibodies including peroxidase coupled secondary antibodies were diluted with blocking buffer except the anti-MBP antibody which was diluted in phosphate buffered saline. The peroxidase substrate 3-amino-9-ethylcarbazole (0.027% w/v; H_2O_2 0.03% v/v) in 0.1 M sodium acetate buffer pH 5.2 was incubated with samples for 20 min at room temperature in the dark. Every

antibody incubation was performed on two slides, of which one was weakly counterstained by haemalum (1 min, Mayer's Haemalum; Merck). The sections were mounted with Kaiser's glycerin–gelatin (Merck) and a cover glass. All the antibodies selected for this study gave a staining pattern on normal tissues consistent with the known antigen distribution. The antibodies were tested for the absence of cross-reactivities with other antigens and the conditions of lowest background were selected.

Histological staining

For histological staining of the myelin, cryostat sections (7 μm thick) were fixed for 1 h in 10% buffered formalin. Slides were washed in double-distilled water and were stained for 1 h in a 0.2% solution of Solochrom-Cyanin (Eriochromcyanin R, Fluka 45560). The sections were washed for 10 min in running tap water and then differentiated in a 10% solution of ammonium iron (III) sulphate for 10–20 s, until the nuclei had lost their colour. A further wash for 10 min in running tap water and twice in double-distilled water followed. Tissues were counterstained with eosin (0.5% w/v in 24% ethanol) for 1 min. For cell nuclear count, some sections were stained with 0.1% (w/v) toluidine blue O (Merck) in 0.1% $Na_2B_4O_7$ solution for 1 min. Sections were finally dehydrated in ethanol, cleared with xylene and mounted with Entellan®neu (Merck) and a cover glass.

Image analysis

A maximum of 50 test fields (84×84 μm each) were analysed from each nerve section using a Zeiss Axiophot microscope and a ×63 oil objective. A maximum of 20 test fields was randomly assigned for a single nerve fascicle. Test fields which contained artifacts or which partially crossed the outside boundaries of a nerve fascicle were excluded. This sampling strategy allowed to analyse ~40% of the total cross-sectional surface of the nerve fascicules from control autopsy tissues and 60–90% of the corresponding value from patient biopsies. A colour image of each test field was captured by a colour CCD camera and the camera signal was decoded with a S-RGB colour decoder into three red–green–blue (RGB) signal channels. The triple signal was digitized and stored on a personal computer (VIDAS 2.1, Kontron Electronic, Carl Zeiss AG, Zürich, Switzerland). Constant values for gain (117) and offset (255) were set to ensure comparable signal intensities. Red–green–blue-decoded colour images were further transferred and compressed on digital audio tapes for later use. The colour images of each test field were discriminated with constant red–green–blue intensity to obtain a binary image of either the zones stained red by the immunohistochemistry, or the regions stained blue by the Solochrome–Cyanin staining. The percentage of antibody- or physical dye-stained surface was defined and estimated as the ratio of the discriminated area divided by the entire test field area and was stored as a single value for each test field. Files of 50 such values per patient and per antibody were stored and converted for mathematical, graphical and statistical operations with various analysis softwares. The number of Solochrome, P_0 and MAG-positive fibres was counted up to 50 digitalized test fields. The ratio of MAG-positive fibres to the total number of myelinated fibres (positive by P_0 or periaxin) was then calculated.

Statistics

The intervariability of the different staining results averaged 30% (range 10–50%) between the three control autopsy specimens. A representative autopsy control with minimal background and high reproducible staining was selected. The mean percentage surface value of six different incubations with each of the 13 antibodies on the reference autopsy control tissue was taken as the general mean control value and was comparable with the mean percentage surface value obtained with the three controls. The intravariability between these six determinations was lower than 10%, except for anti-GalC antibody determinations which showed greater variations. The stained surface of each patient relative to this general mean control is expressed as a percentage normalized to the nerve fascicular area. These percentage values were averaged between all the patients and expressed as relative levels of PNS markers (percentage mean±SE). The bivariate regression plot and the statistical Fischer *R* to *Z* test were used for correlation analysis (StatView software v4.02, Abacus Concepts, Berkeley, Calif., USA).

Double immunostaining

Single and double immunostaining of the nerve biopsies from patients with anti-MAG neuropathy and from a reference autopsy control case were performed on serial sections as described in the immunohistochemistry section above and will be described in detail elsewhere. Briefly, incubation was performed first with D3A2G5 anti-MAG (or D4IE4 anti-P_0 on a separate section) followed by fluorochrome indocarbocyanin 3-conjugated goat anti-mouse IgG (H+L) secondary antibodies. Incubation with antihuman IgM constituted the third step. IgM deposits were demonstrated with μ-chain specific goat antihuman IgM conjugated to the indodicarbocyanin 5 fluorochrome. A Leitz confocal microscope was used for double-channel laser scanning imaging (optical scan z = 0.25 μm). Indocarbocyanin 3 label was recorded as a red false colour, while indodicarbocyanin 5 label was false-colourized green.

Results

Neuropathy features and myelin stain

The clinical, electrophysiological and histological data are consistent with a predominantly demyelinating non-inflammatory neuropathy in all cases (Table 1). The serum

Table 1 *IgM reactivity and neuropathy features in patients with anti-MAG antibodies*

Patient	Sex	Anti-MAG* titre	Clinical data		Nerve studies		
			Symptoms†	Neuropathy feature‡	Peroneal MNCV§	IgM deposits¶	WML#
Bo 1	M	1000	LL	SMNP	25	–	+
Bo 4	M	40000	UL+LL	SMNP	26	Kappa	+
Bo 6	M	100	LL	SNP	Not available	Not done	–
Bo 7	F	50000	LL	SNP	27	Not done	+
Bo 9	F	30000	UL+LL	SMNP	12	Kappa	+
Bo 10	M	10000	LL	SNP	20	Kappa	+
Bo 11	M	60000	LL+tremor	SNP	27	Kappa	+++
Bo 12	M	6000	LL	SNP	19	Kappa	+

*Average of triplicate determinations by Western blot. †Symptoms at neurological examination: UL = upper limbs; LL = lower limbs. ‡SNP = sensory neuropathy; SMNP = sensorimotor neuropathy. §Peroneal MNCV = peroneal motor nerve conduction velocity (m s^{-1}). ¶Direct immunofluorescence study of IgM deposits in myelin sheaths: kappa = positive for kappa light chain; − = negative. #WML = widening of myelin lamellae at ultrastructural examination: + = presence; − = absence.

of all the patients contained anti-MAG IgM antibodies and the anti-MAG titres were highly reproducible both in triplicate determinations by Western blot or single determination by enzyme-linked immunosorbent assay. A sensory neuropathy of the lower limbs predominates in five patients, while three patients have a sensory-motor neuropathy. The nerve conduction velocity ranges from 12 to 27 ms^{-1} and the mean of 22.3 ms^{-1} is similar to the value of 22.9 m s^{-1} reported elsewhere (Nobile-Orazio *et al.*, 1994). Solochrom is a physical myelin stain which binds a complex of ferric ions to the highly negatively charged myelin sheaths and both large and small myelinated fibres are strongly stained blue (Page, 1970) (Fig. 1A). A marked decrease in the number of myelinated fibres is evident in some biopsies of anti-MAG PPN (Fig. 1B). However, for all the biopsies the loss of Solochrom stained fibres does not correlate with the anti-MAG M-IgM titres.

Staining pattern of myelin markers

On control nerves, both the D3A2G5 (Fig. 1C) and the 513 anti-MAG polypeptide mAbs (results not shown) give a similar staining of concentric rings corresponding presumably to the periaxonal collar (arrows, Fig. 1C), paranodal loops and Schmidt–Lanterman incisures (arrowheads, Fig. 1C). By contrast with PPN nerves, both anti-MAG mouse mAbs occasionally and intensely stain the entire thickness of some of the myelin sheaths (arrows, Fig. 1D). The most striking feature of anti-MAG PPN biopsies is the lack of detectable MAG in numerous myelinated fibres. Examination of serial sections confirmed that these MAG negative fibres had a normal pattern of P_0 and MBP expression. Both the anti-MBP mAb (Fig. 1I) and the D4IE4 (Fig. 1E) or the P07 anti-P_0 polypeptide mAbs stain the compact myelin of control nerves; in addition, some axonal staining is seen with the P07 mAb (results not shown). The anti-MBP (Fig. 1J) and anti-P_0 mAbs (Fig. 1F) stain fewer myelinated fibres in PPN. In addition to the known periaxonal localization (Gillespie *et al.*, 1994), anti-periaxin antibodies stain the entire thickness of myelinated fibres and the cytoplasm of myelinating Schwann cells in control (Fig. 1G) and PPN nerves (Fig. 1H). In two cases with anti-MAG PPN (Bo 4 and Bo 9) the anti-periaxin antibodies stain a large number of characteristically very small fibres (arrows, Fig. 1H). This subset of periaxin-positive fibres are not stained by mAbs to P_0 (Fig. 1F) or MBP (Fig. 1J), while we have not been able to establish whether this characteristic subset of very small periaxin-positive fibres are MAG positive or negative. In the PNS the HNK-1 mAb is known to stain glycolipids and numerous glycoproteins including MAG and P_0. On control nerves, HNK-1 strongly stains both large and small myelinated fibres, while it uniformly and weakly stains non-myelinating Schwann cells (Fig. 1K). By contrast, HNK-1 labels non-myelinating Schwann cells of PPN nerves frequently and intensely in areas close to nuclei and axons (arrows, Fig. 1L). Moreover, small Schwann cells sometimes appear as paired striped structures, a pattern typical of clusters of regeneration (Vital and Vallat, 1987) (arrowheads, Fig. 1L).

In each of the eight anti-MAG PPN biopsies the population of myelinated fibres is similarly stained by two different anti-P_0 mAbs. Using the D3A2G5 anti-MAG mAb, however, on average only half of the P_0-positive myelinated fibres contain detectable MAG (Table 2), in a range of 17–83%. By contrast in the reference control nerves 85% of the P_0 myelinated fibres are MAG positive (Table 2). The proportion of MAG-positive fibres to those stained with antibodies to periaxin, another myelin marker, is also reduced in all the anti-MAG PPN specimens (Table 2). While in the reference control nerves there is a similar number of periaxin and P_0-positive fibres, in six anti-MAG PPN patients there are somewhat fewer periaxin-positive than P_0-positive fibres (Table 2), this proportion amounting to 87±3% (range 81–89%). Interestingly, the two patients with a prominent staining of very small fibres, Bo 4 and Bo 9 have a greater number of fibres stained with periaxin than with P_0 (Table 2) with 275% and 105% of the number of P_0-positive fibres, respectively.

Table 2 *Number and proportion of antibody-stained fibres per square millimetre*

Specimen	P_0* ($\times 10^3$)	MAG/P_0 (%)	MAG† ($\times 10^3$)	MAG/pax‡ (%)	Periaxin‡ ($\times 10^3$)	Pax‡/P_0 (%)
Bo 1	6.6	83.1	5.5	93.3	5.9	89.0
Bo 4	1.0	54.1	0.6	19.7	2.8	275.2
Bo 6	3.0	49.7	1.4	57.3	2.5	86.6
Bo 7	5.0	45.6	2.3	46.0	5.0	99.2
Bo 9	3.4	49.7	1.7	47.3	3.6	105.0
Bo 10	2.9	43.3	1.2	53.1	2.3	81.4
Bo 11	8.9	17.4	1.5	20.2	7.6	86.2
Bo 12	7.2	42.6	3.0	51.2	6.0	83.1
Mean±SE§	4.7±0.9	48.0±6.4	2.2±0.5	48.5±8.1	4.5±0.7	113.2±23.3
Control	6.6	85.4	5.6	85.0	6.6	100.5

*D4IE4 anti-Po mAb; †D3A2G5 anti-MAG mAb; ‡anti-periaxin antiserum (pax = periaxin); mean and standard error of the eight PPN nerve biopsies above.

In Patient Bo 4, 80% of the total number of periaxin-positive fibres do not stain for MAG.

Staining pattern of non-myelin markers

Several sural (Fig. 1M), peroneal and femoral control nerves from autopsy are entirely negative with the anti-GFAP mAb (up to a 1:8 dilution), while seven out of the eight anti-MAG PPN nerve biopsy specimens strongly express GFAP in a small subset of non-myelin forming Schwann cells (Fig. 1N). By contrast, a polyclonal antiserum raised against GFAP stains a large subset of Schwann cells in control nerves and considerably more Schwann cells in PPN (*see* quantitative data, below). There is, however, a discrepancy between our results and published data which make use of the polyclonal anti-GFAP antibodies. This antibody has been reported to be negative on human frozen nerve tissue section (Mancardi *et al.*, 1991; Bianchini *et al.*, 1992). In our hands, human nerves obtained from autopsy were positive with this antiserum. Differences in fixation or immunohistochemistry protocols may provide the most likely explanation for this discrepancy. Qualitative analysis of the cellular nuclei stained by toluidine blue indicated an increased cellularity in PPN nerves compared with control nerves. Whether this increased cellularity is accounted for by new myelinating periaxin-positive Schwann cells, non-myelinating GFAP-positive Schwann cells or by fibroblastic proliferation cannot be determined.

Protein S-100, another Schwann cell specific marker, is exclusively localized in the cytoplasm of mature myelinating and non-myelinating Schwann cells of control nerves (arrows, Fig. 1O). The compact myelin is not labelled, while the uncompact myelin regions of Schmidt–Lanterman incisures (arrowheads, Fig. 1O), paranodal loops and the periaxonal collar are labelled on transverse or longitudinal sections (data not shown). In anti-MAG PPN, the overall S-100 staining pattern is similar to control, however, non-myelinating Schwann cells are more prominent (Fig. 1P).

Antibodies to neurofilament 160 kDa, a member of the neuron-specific type IV intermediate filaments, stain exclusively the axoplasm of both myelinated and unmyelinated fibres in control and anti-MAG PPN (results not shown). A minority of myelinated fibres do not stain with this mAb in some anti-MAG PPN biopsy specimens (results not shown).

Quantitative immunohistochemistry

Loss of myelin

A total of 12000 (6800 for anti-MAG PPN and 5200 for control) immunohistochemistry colour images of nerve cryostat sections from anti-MAG PPN and control specimens were processed using the VIDAS image analysis system. The proportion of the nerve fascicular area stained by anti-myelin antibodies is shown in Table 3. The average myelin area which remains in the eight anti-MAG PPN cases is 38% of the reference control myelin surface as estimated by Solochrom staining (Fig. 2). Similar values are obtained using the antibodies to GalC (45%). Quantitative results with anti-GalC antibodies were difficult to interpret because considerable variations were recorded on different occasions (*see* Material and methods). The anti-P_0 (57% and 56%), anti-MBP (54%) and anti-periaxin staining (54%) give a higher estimate of the myelin area which remains in PPN than the results obtained with Solochrom staining (Fig. 2). However, the Solochrom and immunohistochemical staining procedures are not strictly comparable.

Interestingly, although the loss of myelin is prominent in most of the anti-MAG PPN biopsies, the fascicular areas stained by antibodies to the Schwann cell marker protein S100 (96% and 104%) and the axonal neurofilament 160 (102%) are similar in anti-MAG PPN and control specimens (Fig. 2).

Decreased MAG staining level

The average MAG area relative to control (MAG level) which remains in all the anti-MAG PPN cases is smaller than the average area stained with P_0, MBP and periaxin

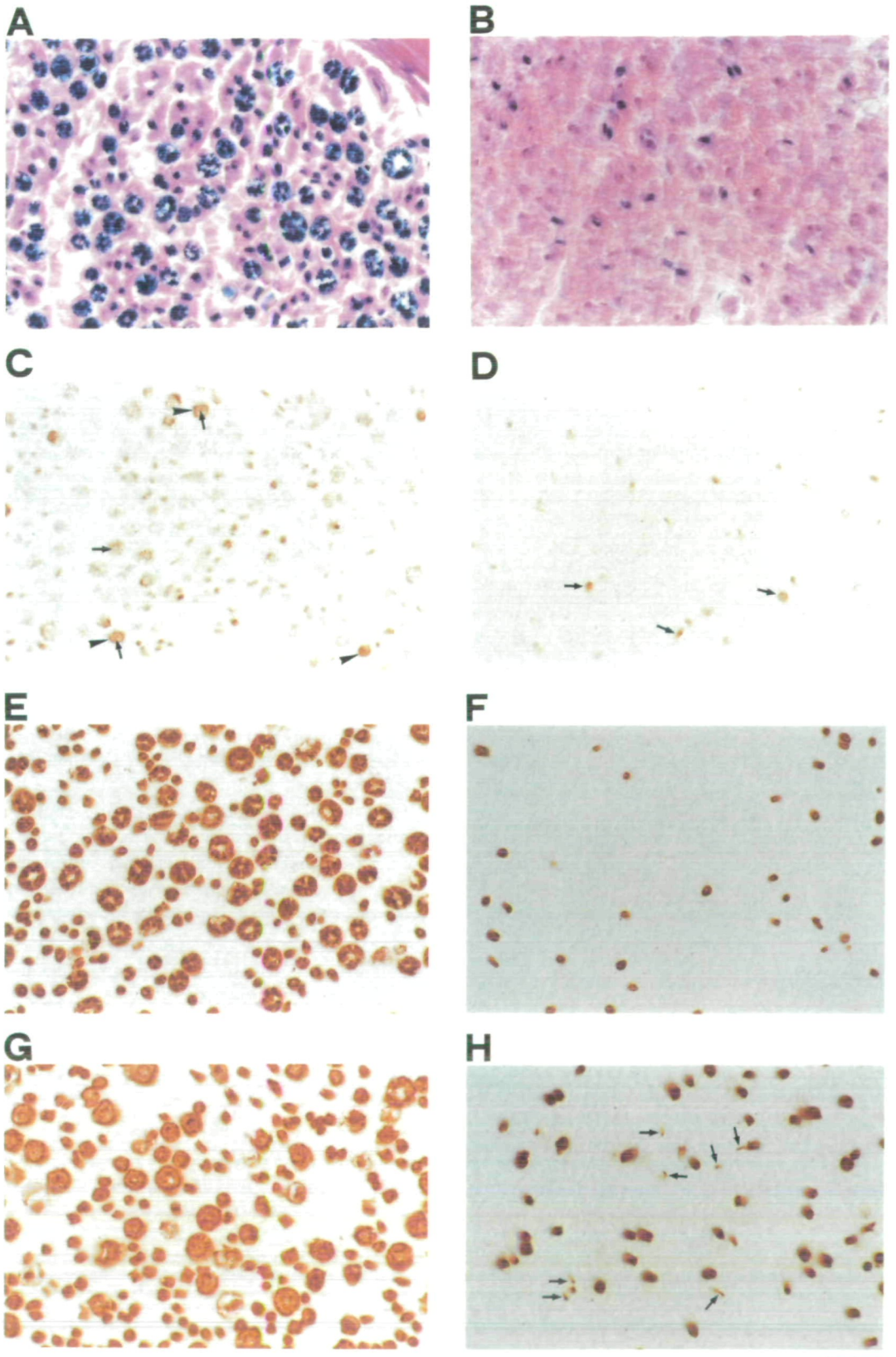

Fig. 1 Photomicrograph of a control sural nerve (**A**, **C**, **E**, **G**, **I**, **K**, **M** and **O**) or a peroneal nerve biopsy from Patient Bo 9 (**B**, **D**, **F**, **H**, **J**, **N** and **P**) or Patient Bo 7 (**L**). Solochrom myelin physical stain and eosin counterstain (**A** and **B**) or immunohistochemical staining with D3A2G5 anti-MAG mAb (**C**, **D**), D4IE4 anti-P0 mAb (**E** and **F**), anti-periaxin antiserum (**G** and **H**), anti-MBP mAb (**I** and **J**), HNK-1 mAb (**K** and **L**), anti-GFAP mAb (**M** and **N**), and anti protein S-100 mAb (**O** and **P**). Haemalum counterstain (**I**, **J**, **M**, **N**, **O** and **P**). In **C**, arrows point to periaxonal staining while arrowhead points to Schmidt–Lanterman incisures. In **D**, arrows point to myelin fibres

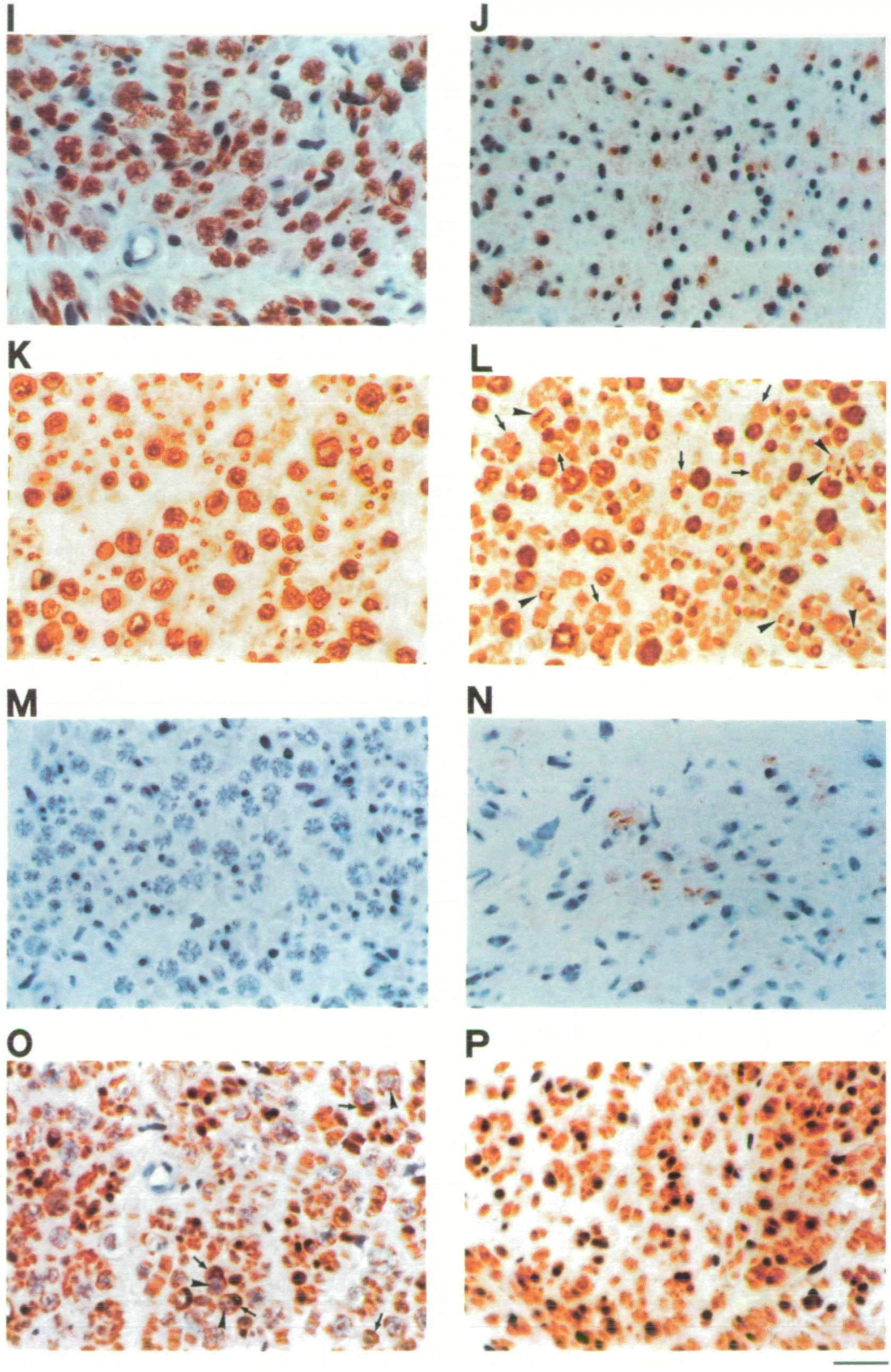

which shows an intense and thick band of MAG staining. In **H**, arrows point to very small fibres which are characteristically periaxin-positive P_0 negative. In **L**, arrows point to areas surrounding nuclei or axons, while arrowheads point to paired stripes structures typical of cluster of regeneration. In **O**, arrows point to cytoplasm of Schwann cells while arrowhead points to Schmidt–Lanterman incisures. The bar represents 25 μm and the same magnification was used for each photomicrograph.

Table 3 *Percentage of the nerve fascicular surface stained by anti-myelin antibodies**

Specimen	MBP†	MAG‡	MAG§	P_0¶	P_0#	Periaxin**
Bo 1	43.7	7.2	2.3	31.5	34.6	47.2
Bo 4	3.3	0.2	0.1	2.0	2.2	6.0
Bo 6	11.1	1.9	1.5	12.6	16.8	14.9
Bo 7	27.6	1.5	1.5	22.8	27.6	23.3
Bo 9	14.6	0.6	0.5	6.7	7.4	11.2
Bo 10	10.4	0.9	0.5	7.5	8.4	9.9
Bo 11	22.9	1.3	0.6	25.0	28.6	41.3
Bo 12	30.6	2.3	1.1	26.0	31.1	28.4
Mean±SE††	20.5±4.7	2.0±0.8	1.0±0.3	16.7±3.9	19.6±4.4	22.8±5.4
Control‡‡	37.8	4.2	4.0	30.0	34.5	42.0

*Nerve sections from PPN and control were stained with anti-myelin antibodies. Between 40 and 50 test fields of 84×84 μm were analysed from each nerve section using the VIDAS image analysis. The percentage of the surface which is stained by antibodies in each nerve fascicule was estimated as the ratio of the discriminated area divided by the entire test field area. These percentage values were then averaged between all the nerve fascicules and expressed as the average percentage of the stained nerve fascicular surface. †130–137 anti-MBP mAb. ‡D3A2G5 anti-MAG mAb. §513 anti-MAG mAb. ¶D4IE4 anti-Po mAb. #P07 anti-Po mAb. **Anti-periaxin antiserum. ††Mean and SE of the eight PPN nerve biopsies above. ‡‡Mean of the reference control nerve determined from six different incubations.

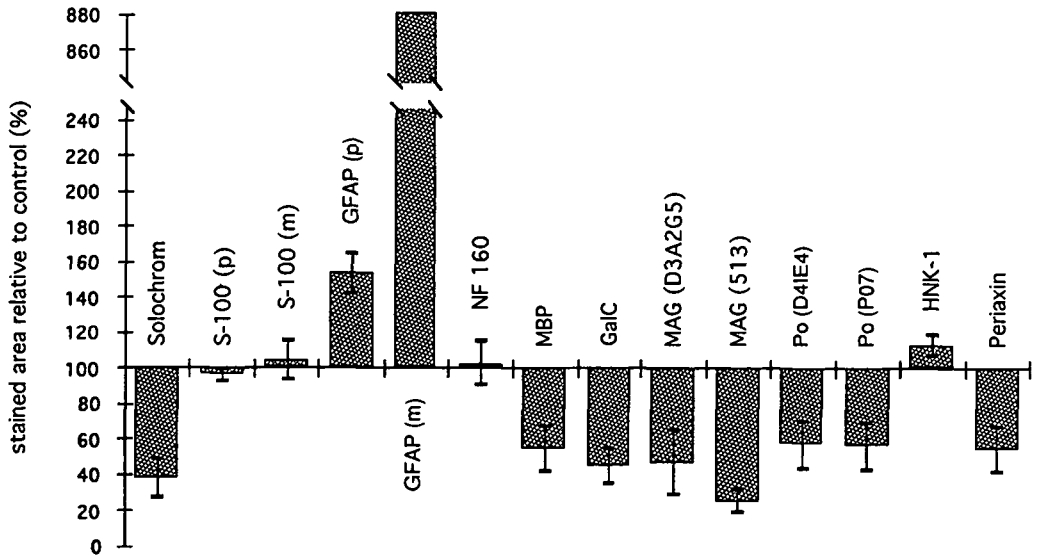

Fig. 2 Relative levels of PNS markers in eight PPN biopsies. The levels correspond to the fractions of nerve fascicular area as determined in Table 2 and are expressed as percent of control. Filled bars represent the difference of these percentage levels between PPN and control tissue. (p) = polyclonal antiserum; (m) = mAb.

antibodies (Fig. 2). The average MAG area normalized to control which is identified with the anti-MAG D3A2G5 mAb (47%) is larger than with the anti-MAG 513 mAb (25%; Fig. 2). This difference is caused by the biopsy specimen of Patient Bo 1, which actually shows a larger stained nerve fascicle area amounting to 169% of control with the D3A2G5 anti-MAG mAb, while the remaining MAG level amounts to 58% of control with the 513 anti-MAG mAb. An independent staining of the Bo 1 specimen and control resulted in more comparable values of 98% and 83% of remaining MAG levels with the D3A2G5 and 513 anti-MAG mAbs, respectively. Another cause is the higher background, weaker and more diffuse staining obtained with the 513 anti-MAG mAb than with the D3A2G5 mAb on control and PPN nerves (data not shown).

Increased GFAP and HNK-1 staining level

The surface staining, with either the polyclonal or monoclonal anti-GFAP antibodies (essentially of non-myelinating Schwann cells), was considerably larger in anti-MAG PPN biopsies than in control tissue and corresponded to 154%, 881% respectively of control (Fig. 2). The apparently large difference between the two antibodies is caused by the control nerves which are positive with the polyclonal but negative with the monoclonal anti-GFAP antibody. Consequently the

ratio of the GFAP level in PPN relative to control nerve is larger with the monoclonal Ab than with the polyclonal (Fig. 2).

The relative areas stained with the HNK-1 mAb, i.e. both non-myelin and myelin forming Schwann cells, were increased in anti-MAG PPN and amounted to 113% of control (Fig. 2).

Correlation between anti-MAG antibody titre and MAG or P_0

An index of MAG distribution in myelinated fibres can be defined as the ratio of the surface stained by the D3A2G5 or 513 anti-MAG mAbs to the area stained by the respective P_0, MBP or periaxin antibodies. In the anti-MAG PPN patients, this relative MAG distribution in myelin shows a significant inverse correlation with the anti-MAG M-IgM antibody titres. A significant correlation factor of r=-0.752 and a probability of $P = 0.029$ is obtained with the D3A2G5 anti-MAG mAb and the D4IE4 anti-P0 mAb surface ratio (Fig. 3). Using the 513 anti-MAG mAb instead of the D3A2G5 mAb results in a similar correlation with anti-MAG M-IgM antibody titres ($r = -0.74$, $P = 0.033$). Highly significant correlations are found between the anti-MAG titres and the MAG distribution relative to either MBP [D3A2G5 mAb: $r = -0.95$, $P < 0.0001$ (Fig. 3); 513 mAb: $r = -0.83$, $P = 0.007$] or periaxin (D3A2G5 mAb: $r = -0.88$, $P = 0.002$; 513 mAb: $r = -0.75$, $P = 0.0029$).

To evaluate the relative density of MAG fibres in myelin we calculated the ratio of fibres stained by the D3A2G5 anti-MAG mAb and the number of myelinated fibres stained by either the D4IE4 or the P07 anti-P_0 mAb or stained by the anti-periaxin antiserum. There is no significant correlation between the anti-MAG antibody titres and the density of MAG fibres relative to either P_0 ($r = -0.472$, $P = 0.252$) or periaxin ($r = -0.661$, $P = 0.0753$). When Patient Bo 4 with a high content of periaxin-positive fibres is excluded from the analysis (Table 2), no significant correlation emerges between the serum anti-MAG titres and the density of MAG fibres relative to either periaxin ($r = -0.626$, $P = 0.1416$) or P_0 ($r = -0.536$, $P = 0.2310$).

There is no correlation between the anti-MAG M-IgM antibody titres and the relative distribution of P_0 in PPN myelin (D4IE4 anti-P_0 /MBP surface ratios: $r = -0.41$, $P = 0.332$; D4IE4 anti-P_0/periaxin surface ratio: $r = -0.32$, $P = 0.463$). There is no correlation either between these titres and the loss of myelin measured as the percentage of nerve fascicular surface relative to control that is stained with anti-P_0, anti-MBP, anti-GalC or anti-periaxin antibodies (as determined in Fig. 2), confirming the previously mentioned negative correlation with the Solochrom stain. No correlation was found between the results with anti-GFAP or HNK-1 mAbs and the anti-MAG M-IgM antibody titres.

Immunofluorescence staining

Double immunostaining for IgM autoantibodies and MAG in PPN nerves revealed four different populations of myelinated fibres (Fig. 4). The first population contains strongly stained MAG fibres without IgM deposits. The second and third populations include IgM positive myelin fibres with strong or weak MAG labelling, respectively. In this population of fibres, the IgM paraprotein was deposited as a thin ring at the periphery of myelinated fibres. The fourth population consist of IgM-positive fibres without MAG staining in which IgM are deposited either as thick rings at the periphery or in the entire thickness of myelin sheaths.

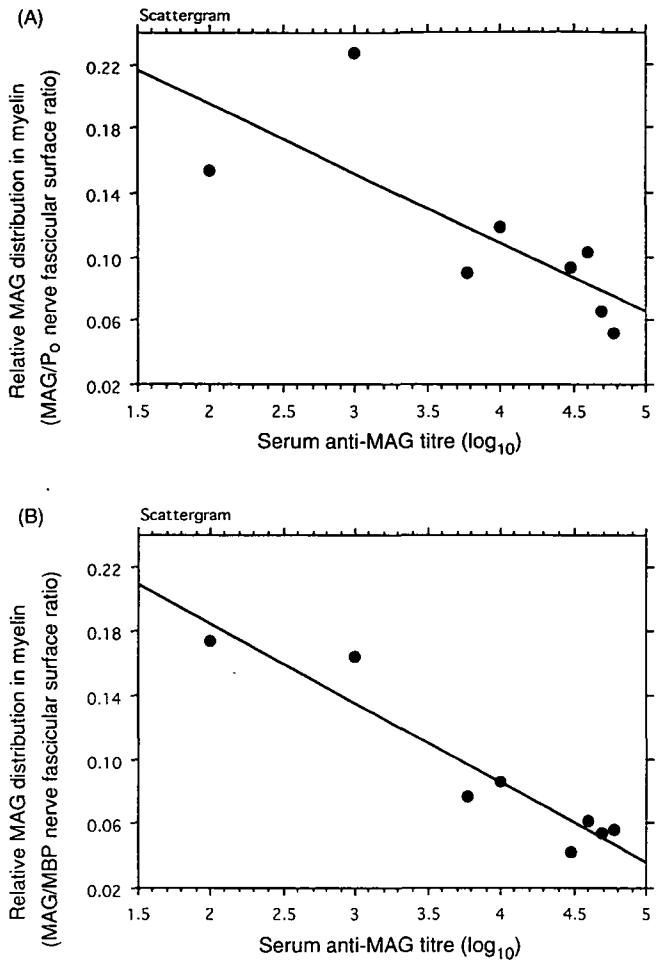

Fig. 3 Correlation of MAG distribution in PPN myelin with serum anti-MAG M-IgM titres. The relative MAG distribution in the myelin of each PPN biopsy was determined as the ratio of the nerve fascicular area stained with the D3A2G5 anti-MAG mAb relative to either the D4IE4 anti-P_0 mAbs (**A**) or the 130–137 anti-MBP mAbs (**B**).

Discussion

The anti-MAG M-IgM neuropathy is characterized by a distally pronounced progressive chronic demyelination (Mendell *et al.*, 1985). The circulating anti-MAG M-IgM autoantibodies make deposits that characteristically outline the outer aspect of some of the remaining myelin sheaths and alter their ultrastructure (King and Thomas, 1984; Mendell *et al.*, 1985). Our biopsy material obtained from

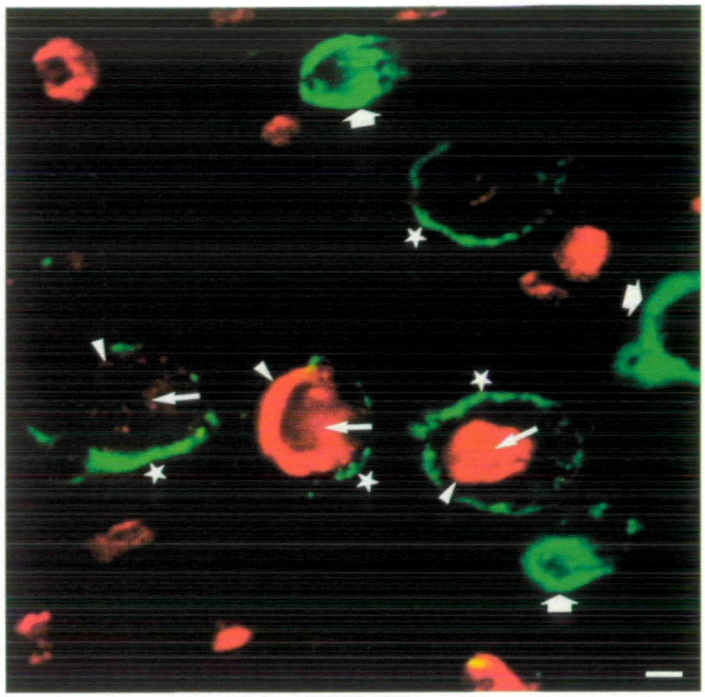

Fig. 4 Photomicrograph of a peroneal nerve biopsy from Patient Bo 12. Double-immunofluorescence staining with D3A2G5 anti-MAG mAb (red label) and human IgM deposits (green label). Four large myelinated fibres are stained by anti-MAG and anti-IgM antibodies without colour overlapping (stars). Note the weaker MAG staining in two of these fibres. Massive IgM deposits are present in three additional myelinated fibres lacking a MAG staining (large arrows). Small arrows point to periaxonal staining while arrowheads point to Schmidt–Lanterman incisures. The bar represents 2.5 μm.

eight patients with anti-MAG M-IgM neuropathy shows variable loss of myelinated fibres, a finding comparable with previous reports (Mendell *et al.*, 1985; Vital *et al.*, 1989). The reduction of myelinated fibres seen in these biopsies with the Solochrom myelin stain correlates with the decrease of fibres labelled with antibodies to P_0, MBP and periaxin and, to a lesser degree, MAG. There is also a good agreement between the density of P_0^+ or MBP^+ fibres and the density of myelinated fibres determined by electron microscopy of ultrathin sections from separate tissue blocks (data not shown).

An intriguing result of our study of anti-MAG PPN nerves is the lack of detectable MAG staining in a large population of remaining myelinated fibres. Accordingly there is a larger decrease of MAG-positive staining fascicular area than observed with other myelin markers by quantitative immunohistochemistry. The inability to detect MAG in a large population of myelinated fibres is not attributable to a masking effect by M-IgM bound to MAG carbohydrate epitopes because MAG is detectable with two different mouse mAbs which recognize each a distinct MAG polypeptide epitope. Moreover, two-colour immunofluorescence confocal microscopy studies of PPN nerves show the presence of MAG and IgM deposits in some myelin fibres while MAG negative myelinated fibres are associated with extensive IgM deposits. In the former population of myelinated fibres, MAG staining appears as concentric rings corresponding presumably to the periaxonal collar (inner ring) and Schmidt–Lanterman incisure (outer ring) while IgM autoantibodies are deposited at the periphery of the myelinated fibres without overlapping the MAG staining. Interestingly, MAG staining intensities ranging from weak to strong (comparable with control nerves or with myelinated fibre devoid of IgM in PPN nerves) were associated with a thin ring of IgM deposits. This decreased MAG staining could be the result of reduced MAG expression. By contrast, myelinated fibres devoid of MAG staining were often associated with thick IgM deposits either at the periphery or in the entire thickness of the myelin sheaths.

The normal staining pattern observed with the myelin markers P_0, MBP and periaxin in myelin sheaths devoid of detectable MAG represents an unexpected finding. Many of these MAG^- P_0^+ myelinated fibres could be functionally normal in PPN: (i) the ratio of MAG-positive to P_0-positive fibres does not correlate with the loss of myelinated fibres; (ii) nerve conduction velocities were normal (Montag *et al.*, 1994) and no loss of myelinated fibres occurred in young mice with disrupted MAG genes (Li *et al.*, 1994; Montag *et al.*, 1994); (iii) the axons enwrapped by the MAG^- P_0^+ fibres seem unaffected as the nerve fascicular surface stained by antibodies to neurofilament 160 remains unchanged between the PPN and control nerves. This selective loss of MAG in myelinated fibres could result either from an antibody-mediated antigenic modulation or from a down-regulation of gene expression and may represent a chronic state in the anti-MAG PPN. As a long-term effect of MAG loss both axon and myelin degeneration can, however, occur, resulting in a very slowly progressive neuropathy. Our results are compatible with the notion that MAG plays a major role in the maintenance of myelin integrity rather than in its formation. This has been shown recently to be the case in old mice with disrupted MAG genes (Fruttiger *et al.*, 1995), where both axonal and myelin degeneration is taking place.

Another important observation of this study is that the circulating anti-MAG autoantibody titres show an inverse correlation with the relative distribution of MAG in the remaining myelin sheaths. By contrast, the proportion of MAG to P_0-positive myelinated fibres does not correlate with the patients' serum anti-MAG autoantibody titres. The functional consequence of the relationship between the serum anti-MAG antibody titres and the distribution of MAG in myelin suggests that the binding of anti-MAG M-IgM autoantibodies to MAG could result in an altered pattern of MAG expression. The autoantibodies in PPN might also affect the size of the remaining MAG^+ fibres and, at present, it cannot be excluded that they exert at least some of their effects by binding to other myelin components in addition to MAG. Both the selective loss of MAG and the qualitative changes of MAG staining in the remaining myelin argue for a disregulation of MAG expression in PPN. In contrast to

MAG, the P_0 distribution in the remaining PPN myelin sheaths does not seem to be affected directly by the presence of the anti-MAG M-IgM autoantibodies, although both MAG and P_0 carry the same HNK-1 carbohydrate epitopes. This is consistent with reports showing a higher apparent avidity of anti-MAG M-IgM antibodies for the multiple HNK-1 carbohydrate epitopes of MAG than for the unique P_0 epitope (Burger *et al.*, 1990; Brouet *et al.*, 1992; Ogino *et al.*, 1994).

The localization of the four myelin markers MAG, P_0, MBP and GalC in human control peripheral nerves is consistent with previous reports (Trapp, 1990; Mezei, 1993; Poduslo, 1993; Martini, 1994). In particular, the concentric rings of MAG staining seen in cross-sections of control nerves is in agreement with the localization of MAG in uncompact myelin, mainly in Schmidt–Lanterman incisures, paranodal loops and in the periaxonal region where it is believed to be involved in the tight apposition of the axolemma and the inner lip of the myelinating Schwann cell (Trapp and Quarles, 1982; Trapp *et al.*, 1984). In contrast to this pattern, the localization of MAG in PPN nerves occasionally differs from the typical concentric rings of control nerves. In occasional biopsies, an intense and thick band of MAG staining is observed to varying degrees in some of the myelinated fibres. One interpretation of this observation is that there could be an accumulation of fibres with multiple layers of non-compacted MAG^+ Schwann cell membranes (Trapp and Quarles, 1984). Theoretically the binding of the anti-MAG M-IgM could perturb adhesion properties of MAG to a presumptive receptor and thereby produce ultrastructural changes. Alternatively, the autoantibodies could perturb signalling functions involving molecules associated with MAG, such as the Fyn protein tyrosine kinase. Indeed, disruption of the Fyn kinase gene in mice leads to hypomyelination (Umemori *et al.*, 1994).

It has been suggested that periaxin could associate with the cytoplasmic domain of MAG at the periaxonal collar of myelinating Schwann cell where it might be important for the regulation of axon-Schwann cell interactions (Gillespie *et al.*, 1994). Using the same anti-periaxin antiserum we find staining throughout the entire thickness of myelin in the nerves of both newborn rats (data not shown) and adult human controls. These observations indicate that the expression of MAG is not coordinately linked with that of periaxin in PPN nerves: on average, 50% of periaxin-positive fibres lacked MAG in six out of eight anti-MAG PPN cases, and in the remaining two anti-MAG PPN cases there was an increased population of very small fibres with periaxin but not P_0 or MBP staining. The latter may represent either new myelinating fibres or remyelinating fibres since P_0 and MBP are markers of late myelination, while periaxin may be one of the first myelin protein expressed in myelinating Schwann cells (P. Brophy, personal communication). The fact that more nuclei are found in PPN nerves and more surface is stained by anti-GFAP mAbs is consistent with a proliferation of non-myelin forming Schwann cells. Conceivably, periaxin might be the first marker expressed in new or regenerating myelin, followed by MAG and later on by P_0 and MBP. The presence of $periaxin^+P_0^-$ fibres is consistent with an increased potential for remyelination or new myelin formation in this disease.

The apparent loss of myelinated fibres in anti-MAG PPN nerves occurs concomitantly with a prominent increase of the GFAP marker of non-myelin forming Schwann cells (Mokuno *et al.*, 1989; Mancardi *et al.*, 1991; Bianchini *et al.*, 1992; Feinstein *et al.*, 1992). This increase is specific to PPN since it was absent in other neuropathies such as Charcot–Marie–Tooth type 1A, hereditary neuropathy with liability to pressure palsies, Guillain–Barré syndrome or chronic inflammatory demyelinating polyradiculoneuropathy (J.-M. Gabriel, B. Erne and A. J. Steck, unpublished results). The increased number of nuclei as well as the presence of Schwann cell hypertrophy in some of the PPN nerves biopsies are consistent with varying degrees of gliosis. In addition to GFAP, we also observed an increased expression of the HNK-1 marker in anti-MAG PPN nerves. Among the many molecules containing the HNK-1 epitope, MAG and P_0 are not involved (this study), while neuron cell adhesion molecule could be a possible candidate for the HNK-1 up-regulation in the MAG negative fibres since neuron cell adhesion molecule was found to be up-regulated in MAG knock-out mice (Montag *et al.*, 1994). We have some preliminary evidence that neuron cell adhesion molecule is indeed up-regulated in PPN nerves (J.-M. Gabriel, B. Erne and A. J. Steck, unpublished results).

Conclusion

The results from this study provide novel evidence that MAG may be an important functional target of the anti-MAG M-IgM autoantibodies in PPN. In addition, original features of this disease have been identified by phenotypic marker analysis which could not be detected with morphological histopathological techniques. Future investigations should attempt to delineate the populations of demyelinating and remyelinating fibres in anti-MAG M-IgM paraproteinaemic polyneuropathy as a prerequisite step to understanding the mechanisms of demyelination in PPN.

Acknowledgements

We wish to thank Mrs Fabrizia Ferracin for myelin preparations and western blots of anti-MAG antibodies, Dr Juan Archelos (Neurology Clinic, Würzburg, Germany) for the gift of the P07 anti-P_0 mAb and Dr Peter Brophy (University of Stirling, UK) for the gift of antisera to periaxin. We acknowledge the help of Dr Martin Oberholzer (Department of Diagnostic Morphometry, University of Basel) for initial use of his VIDAS system, Drs Jürg Ulrich and Alphonse Probst (Department of Neuropathology, University of Basel) for providing us with control autopsy nerve tissues and Dr Lucas Landmann (Deparment of Anatomy, University of Basel) for the confocal microscopy

imaging. We thank Drs Peter Brophy and Jürg Ulrich for helpful discussions and critical reading of the manuscript. J.-M.G. was supported by a fellowship from the Swiss National Science Foundation and B.E. by the Swiss Multiple Sclerosis Society and University Hospital, Basel.

References

Abo T, Balch CM. A differentiation antigen of human NK and K cells identified by a monoclonal antibody (HNK-1). J Immunol 1981; 127: 1024–9.

Archelos JJ, Roggenbuck K, Schneider-Schaulies J, Linington C, Toyka KV, Hartung HP. Production and characterization of monoclonal antibodies to the extracellular domain of P_0. J Neurosci Res 1993; 35: 46–53.

Bergoffen J, Scherer SS, Wang S, Scott MO, Bone LJ, Paul DL, et al. Connexin mutations in X-linked Charcot–Marie–Tooth disease. Science 1993; 262: 2039–42.

Bianchini D, De Martini I, Cadoni A, Zicca A, Tabaton M, Schenone A, et al. GFAP expression of human Schwann cells in tissue culture. Brain Res 1992; 570: 209–17.

Bollensen E, Steck AJ, Schachner M. Reactivity with the peripheral myelin glycoprotein P_0 in serum from patients with monoclonal IgM gammopathy and polyneuropathy. Neurology 1988; 38: 1266–70.

Braun PE, Frail DE, Latov N. Myelin-associated glycoprotein is the antigen for a monoclonal IgM in polyneuropathy. J Neurochem 1982; 39: 1261–5.

Brouet JC, Mariette X, Chevalier A, Hauttecoeur B. Determination of the affinity of monoclonal human IgM for myelin-associated glycoprotein and sulfated glucuronic paragloboside. J Neuroimmunol 1992; 36: 209–15.

Burger D, Simon M, Perruisseau G, Steck AJ. The epitope(s) recognized by HNK-1 antibody and IgM paraprotein in neuropathy is present on several N-linked oligosaccharide structures on human P_0 and myelin-associated glycoprotein. J Neurochem 1990; 54: 1569–75.

Debus E, Weber K, Osborn M. Monoclonal antibodies specific for glial fibrillary acidic (GFA) protein and for each of the neurofilament triplet polypeptides. Differentiation 1983; 25: 193–203.

Feinstein DL, Weinmaster GA, Milner RJ. Isolation of cDNA clones encoding rat glial fibrillary acidic protein: expression in astrocytes and in Schwann cells. J Neurosci Res 1992; 32: 1–14.

Frail DE, Edwards AM, Braun PE. Molecular characteristics of the epitope in myelin-associated glycoprotein that is recognized by a monoclonal IgM in human neuropathy patients. Mol Immunol 1984; 21: 721–5.

Fruttiger M, Montag D, Schachner M, Martini R. Crucial role for the Myelin-associated glycoprotein in the maintenance of axon-myelin integrity. Eur J Neurosci 1995; 7: 511–15.

Gillespie CS, Sherman DL, Blair GE, Brophy PJ. Periaxin, a novel protein of myelinating Schwann cells with a possible role in axonal ensheathment. Neuron 1994; 12: 497–508.

Ilyas AA, Quarles RH, MacIntosh TD, Dobersen MJ, Trapp BD, Dalakas MC, et al. IgM in a human neuropathy related to paraproteinemia binds to a carbohydrate determinant in the myelin-associated glycoprotein and to a ganglioside. Proc Natl Acad Sci USA 1984; 81: 1225–9.

Kaku DA, England JD, Sumner AJ. Distal accentuation of conduction slowing in polyneuropathy associated with antibodies to myelin-associated glycoprotein and sulphated glucuronyl paragloboside. Brain 1994; 117: 941–7.

King RHM, Thomas PK. The occurrence and significance of myelin with unusually large periodicity. Acta Neuropathol (Berl) 1984; 63: 319–29.

Lach B, Rippstein P, Atack D, Afar DE, Gregor A. Immunoelectron microscopic localization of monoclonal IgM antibodies in gammopathy associated with peripheral demyelinative neuropathy. Acta Neuropathol (Berl) 1993; 85: 298–307.

Li C, Tropak MB, Gerlai R, Clapoff S, Abramow-Newerly W, Trapp B, et al. Myelination in the absence of myelin-associated glycoprotein. Nature 1994; 369: 747–50.

Mancardi GL, Cadoni A, Tabaton M, Schenone A, Zicca A, De Martini I, et al. Schwann cell GFAP expression increases in axonal neuropathies. J Neurol Sci 1991; 102: 177–83.

Martini R. Expression and functional roles of neural cell surface molecules and extracellular matrix components during development and regeneration of peripheral nerves. [Review]. J Neurocytol 1994; 23: 1–28.

McGarry RC, Helfand SL, Quarles RH, Roder JC. Recognition of myelin-associated glycoprotein by the monoclonal antibody HNK-1. Nature 1983; 306: 376–8.

Mendell JR, Sahenk Z, Whitaker JN, Trapp BD, Yates AJ, Griggs RC, et al. Polyneuropathy and IgM monoclonal gammopathy: studies on the pathogenetic role of anti-myelin-associated glycoprotein antibody. Ann Neurol 1985; 17: 243–54.

Mezei C. Myelination in the peripheral nerve during development. In: Dyck PJ, Thomas PK, Griffin JW, Low PA, Poduslo JF, editors. Peripheral neuropathy. 3rd ed. Philadelphia: W. B. Saunders, 1993: 267–81.

Miller SL, Pleasure D, Herlyn M, Atkinson B, Ernst C, Tachovsky TG, et al. Production and characterization of monoclonal antibodies to peripheral and central nervous system myelin. J Neurochem 1984; 43: 394–400.

Mokuno K, Kamholz J, Behrman T, Black C, Sessa M, Feinstein D, et al. Neuronal modulation of Schwann cell glial fibrillary acidic protein (GFAP). J Neurosci Res 1989; 23: 396–405.

Monaco S, Bonetti B, Ferrari S, Moretto G, Nardelli E, Tedesco F, et al. Complement-mediated demyelination in patients with IgM monoclonal gammopathy and polyneuropathy. N Engl J Med 1990; 322: 649–52.

Montag D, Giese KP, Bartsch U, Martini R, Lang Y, Blüthmann H, et al. Mice deficient for the myelin-associated glycoprotein show subtle abnormalities in myelin. Neuron 1994; 13: 229–46.

Nobile-Orazio E, Manfredini E, Carpo M, Meucci N, Monaco S, Ferrari S, et al. Frequency and clinical correlates of anti-neural IgM antibodies in neuropathy associated with IgM monoclonal gammopathy. Ann Neurol 1994; 36: 416–24.

Ogino M, Tatum AH, Latov N. Affinity studies of human anti-MAG antibodies in neuropathy. J Neuroimmunol 1994; 52: 41–6.

Page KM. Histological methods for peripheral nerves—Part I. J Med Lab Technol 1970; 27: 1–17.

Poduslo JF. Regulation of myelin gene expression in the peripheral nervous system. In: Dyck PJ, Thomas PK, Griffin JW, Low PA, Poduslo JF, editors. Peripheral neuropathy. 3rd ed. Philadelphia: W. B. Saunders, 1993: 282–9.

Poltorak M, Sadoul R, Keilhauer G, Landa C, Fahrig T, Schachner M. Myelin-associated glycoprotein, a member of the L2/HNK-1 family of neural cell adhesion molecules, is involved in neuron-oligodendrocyte and oligodendrocyte-oligodendrocyte interaction. J Cell Biol 1987; 105: 1893–9.

Schuller-Petrovic S, Gebhart N, Lassmann H, Rumpold H, Kraft D. A shared antigenic determinant between natural killer cells and nervous tissue. Nature 1983; 306: 179–81.

Steck AJ, Murray N, Meier C, Page N, Perruisseau G. Demyelinating neuropathy and monoclonal IgM antibody to myelin-associated glycoprotein. Neurology 1983; 33: 19–23.

Tatum AH. Experimental paraprotein neuropathy, demyelination by passive transfer of human IgM anti-myelin-associated glycoprotein. Ann Neurol 1993; 33: 502–6.

Trapp BD. Myelin-associated glycoprotein. Location and potential functions. [Review]. Ann N Y Acad Sci 1990; 605: 29- 43.

Trapp BD, Quarles RH. Presence of the myelin-associated glycoprotein correlates with alterations in the periodicity of peripheral myelin. J Cell Biol 1982; 92: 877–82.

Trapp BD, Quarles RH. Immunocytochemical localization of the myelin-associated glycoprotein. Fact or artifact? J Neuroimmunol 1984; 6: 231–49.

Trapp BD, Quarles RH, Suzuki K. Immunocytochemical studies of quaking mice support a role for the myelin-associated glycoprotein in forming and maintaining the periaxonal space and periaxonal cytoplasmic collar of myelinating Schwann cells. J Cell Biol 1984; 99: 594–606.

Trojaborg W, Galassi G, Hays AP, Lovelace RE, Alkaitis M, Latov N. Electrophysiologic study of experimental demyelination induced by serum of patients with IgM M proteins and neuropathy. Neurology 1989: 39: 1581–6.

Umemori H, Sato S, Yagi T, Aizawa S, Yamamoto T. Initial events of myelination involve Fyn tyrosine kinase signalling. Nature 1994; 367: 572–6.

Vital C, Vallat J-M. Elementary parenchymal lesions. In: Vital C, Vallat J-M, editors. Ultrastructural study of the human diseased peripheral nerve. New York: Elsevier, 1987: 27–92.

Vital A, Vital C, Julien J, Baquey A, Steck AJ. Polyneuropathy associated with IgM monoclonal gammopathy. Immunological and pathological study in 31 patients. Acta Neuropathol (Berl) 1989; 79: 160–7.

Weber K, Shaw G, Osborn M, Debus E, Geisler N. Neurofilaments, a subclass of intermediate filaments: structure and expression. Cold Spring Harb Symp Quant Biol 1983; 48: 717–29.

Received November 10, 1995. Revised January 24, 1996. Accepted February 6, 1996